AASLD
AMERICAN ASSOCIATION FOR
THE STUDY OF LIVER DISEASES

Glycine-β-muricholic acid antagonizes the intestinal farnesoid X receptor–ceramide axis and ameliorates NASH in mice

Jie Jiang[1,2] | Yuandi Ma[2,3] | Yameng Liu[2] | Dasheng Lu[4] | Xiaoxia Gao[4] |
Kristopher W. Krausz[4] | Dhimant Desai[5] | Shantu G. Amin[5] |
Andrew D. Patterson[6] | Frank J. Gonzalez[4] ⓘ | Cen Xie[1,2,3,4] ⓘ

[1]School of Chinese Materia Medica, Nanjing University of Chinese Medicine, Nanjing, China

[2]State Key Laboratory of Drug Research, Shanghai Institute of Materia Medica, Chinese Academy of Sciences, Shanghai, China

[3]University of Chinese Academy of Sciences, Beijing, China

[4]Department of Pharmacology, College of Medicine, The Pennsylvania State University, Hershey, Pennsylvania, USA

[5]Laboratory of Metabolism, Center for Cancer Research, National Cancer Institute, National Institutes of Health, Bethesda, Maryland, USA

[6]Department of Veterinary and Biomedical Sciences and the Center for Molecular Toxicology and Carcinogenesis, The Pennsylvania State University, University Park, Pennsylvania, USA

Correspondence
Frank J. Gonzalez, Laboratory of Metabolism, Center for Cancer Research, National Cancer Institute, National Institutes of Health, Bethesda, MD 20892, USA.
Email: gonzalef@mail.nih.gov

Cen Xie, State Key Laboratory of Drug Research, Shanghai Institute of Materia Medica, Chinese Academy of Sciences, Shanghai 201203, China.
Email: cenxie@simm.ac.cn

Abstract

Nonalcoholic steatohepatitis (NASH) is a rapidly developing pathology around the world, with limited treatment options available. Some farnesoid X receptor (FXR) agonists have been applied in clinical trials for NASH, but side effects such as pruritus and low-density lipoprotein elevation have been reported. Intestinal FXR is recognized as a promising therapeutic target for metabolic diseases. Glycine-β-muricholic acid (Gly-MCA) is an intestine-specific FXR antagonist previously shown to have favorable metabolic effects on obesity and insulin resistance. Herein, we identify a role for Gly-MCA in the pathogenesis of NASH, and explore the underlying molecular mechanism. Gly-MCA improved lipid accumulation, inflammatory response, and collagen deposition in two different NASH models. Mechanistically, Gly-MCA decreased intestine-derived ceramides by suppressing ceramide synthesis–related genes via decreasing intestinal FXR signaling, leading to lower liver endoplasmic reticulum (ER) stress and proinflammatory cytokine production. The role of bile acid metabolism and adiposity was excluded in the suppression of NASH by Gly-MCA, and a correlation was found between intestine-derived ceramides and NASH severity. This study revealed that Gly-MCA, an intestine-specific FXR antagonist, has beneficial effects on NASH by reducing ceramide levels

---

Jie Jiang and Yuandi Ma contributed equally to this work.

circulating to liver via lowering intestinal FXR signaling, and ceramide production, followed by decreased liver ER stress and NASH progression. Intestinal FXR is a promising drug target and Gly-MCA a novel agent for the prevention and treatment of NASH.

INTRODUCTION

Nonalcoholic fatty liver disease (NAFLD) is the most prevalent cause of chronic liver diseases, closely associated with obesity, type 2 diabetes, hypertension, and dyslipidemia.[1] NAFLD can be divided histologically into nonalcoholic fatty liver (NAFL) and nonalcoholic steatohepatitis (NASH).[2] NAFL is a benign form of NAFLD with excess fat in the liver and no hepatocellular damage,[3] whereas NASH is a progressive form of this disease, characterized with ballooning, lobular inflammation, and deposition of collagen fibers in addition to steatosis.[4] NASH can eventually progress to cirrhosis and hepatocellular carcinoma. The multiple-hit hypothesis provides a more accurate and widely accepted explanation of NASH. Initial hits lead to the development of simple steatosis, following hepatocyte inflammation and apoptosis, resulting in mitochondrial dysfunction, oxidative stress, lipid peroxidation, and Kupffer cell activation.[5] NASH is a heavy burden on the public health system, and options for pharmacologic therapy targeting NASH remain extremely limited.[5,6]

Farnesoid X receptor (FXR), a bile acid-activated nuclear receptor, regulates many biological processes, including bile acid homeostasis, and lipid and glucose metabolism.[7] Recently, extensive studies have suggested that a lack of intestinal FXR protects mice from obesity, insulin resistance, and NAFLD, thus confirming the involvement of intestinal FXR in the pathogenesis of metabolic diseases.[8–10] Therefore, it is imperative that we elucidate the effects of intestinal FXR on the development of NASH, enabling the development of new pharmacological treatments for this disorder.

It was reported that tauro-beta-muricholic acid (T-β-MCA) antagonizes intestinal FXR signaling, correlated with its improved metabolic function.[11,12] Nevertheless, T-β-MCA does not act as a long-acting inhibitor of intestine-specific FXR *in vivo*, in that it is rapidly hydrolyzed by bacterial bile salt hydrolase (BSH). Glycine-β-muricholic acid (Gly-MCA), a derivative of T-β-MCA, was identified by molecular modeling as a FXR antagonist that is resistant to hydrolysis by BSH.[8] Gly-MCA improved glucose and lipid metabolism, and thus alleviated obesity-related metabolic disorders.[13] Nevertheless, the therapeutic effects of Gly-MCA on NASH remain largely undetermined.

In the present study, Gly-MCA was found to ameliorate NASH manifested in reduced hepatic lipid accumulation, inflammation, and fibrogenesis, exerting its action on the intestinal FXR-ceramide axis rather than bile acid metabolism in the ileum. Taken together, Gly-MCA or another gut-specific FXR antagonist could, to be a promising agent for preventing or treating NASH due to its low hepatotoxicity and significant therapeutic effects.

METHODS

Reagents and materials

Gly-MCA was synthesized by a previously described method.[8] Bile acid standards were obtained from Steraloids, Inc. or Sigma-Aldrich. Ceramide standards (C16:0, C17:0, C18:0, C20:0, C22:0, C24:0, and C24:1) were purchased from Avanti Polar Lipids. Low-fat diet (LFD; D12450B), Amylin liver NASH model diet (AMLN diet; D09100301), methionine-choline-sufficient diet (MCS; A02082003B), and methionine and choline-deficient diet (MCD; A02082002B) were purchased from Research Diet.

Animal studies

Control (*Fxr*^{fl/fl}) mice and intestine-specific *Fxr*-null (*Fxr*[ΔIE]) were on a C57BL/6N genetic background (backcrossed over 10 generations).[14] Male C57BL/6N mice aged 6 weeks were purchased from Charles River Laboratories or HuaFukang BioScience Company. Animal procedures were approved by the National Cancer Institute Animal Care and Use Committee and the Animal Ethics Committee of Shanghai Institute of Materia Medica. For all mice, the circadian rhythm was 12 h, and access to water and food was *ad libitum*. Oral administration of Gly-MCA was based on the addition of Gly-MCA (10 mg kg^{-1} day^{-1}) to bacon-flavored dough pills. For the therapy of NASH, Gly-MCA (10 mg kg^{-1} day^{-1}) was administered to 8-week-old male C57BL/6N mice for 8 weeks, after feeding either a LFD or AMLN diet for 0 to 12 weeks. To determine whether Gly-MCA was intestinally FXR-dependent, 6–8-week-old male *Fxr*^{fl/fl} and *Fxr*[ΔIE] mice fed an AMLN diet for 12 weeks were orally administered vehicle or Gly-MCA (10 mg kg^{-1} day^{-1}) for 8 weeks. The 8-week-old mice were fed an MCS or MCD diet for 4 weeks and were

simultaneously or immediately administered vehicle pills or Gly-MCA pills ($10\,mg\,kg^{-1}\,day^{-1}$) to rule out the effect of adiposity. The 6–8-week-old male $Fxr^{fl/fl}$ and $Fxr^{\Delta IE}$ mice fed an MCD diet were orally administered vehicle or Gly-MCA ($10\,mg\,kg^{-1}\,day^{-1}$) pills simultaneously for 4 weeks to determine the role of intestinal FXR in MCD diet–induced NASH. Mice on AMLN diet received vehicle or C16:0 ceramide at a dose of $10\,mg\,kg^{-1}\,day^{-1}$ via intraperitoneal injection every other day for 3 weeks in the ceramide supplementation study.

Clinical chemistry measurements

As directed by the manufacturer (Nanjing Jiancheng Bioengineering Institute or Bioassay Systems), levels of serum alanine aminotransferase (ALT), aspartate aminotransferase (AST), and hepatic lipids (triglycerides [TG] and free cholesterol) were measured.

Liver histology analysis

Frozen sections were stained for Oil Red O, and paraffin-embedded sections were stained for hematoxylin and eosin (H&E), Masson, and Sirius Red according to standard protocols. The slides were observed under a light microscope. Livers of each mouse were examined from at least three different discontinuous sections.

Quantitative real-time polymerase chain reaction

Total RNA was isolated and converted to complementary DNA using TRIzol Reagent (Invitrogen), followed with PrimeScript reverse transcriptase (Takara Bio). Quantitative real-time polymerase chain reactions (PCRs) were running with SYBR Premix Ex Taq (Takara Bio) and a real-time PCR detection system CFX384. Table S1 presents quantitative real-time PCR primer sequences.

Ceramide and bile acid analysis

In serum lipidomics, the serum samples were extracted with chloroform–methanol solution containing C17:0 ceramide. After separation, drying, and redissolution, the samples were injected for analysis. In ileal and hepatic lipidomics, tissue samples were homogenized with methanol–H_2O solution and then extracted using chloroform containing C17:0-ceramide. Samples could be injected for analysis after homogenate, shock, incubation, separation, drying, and redissolution. All samples were separated by an Acquity UPLC CSH C18

column (Waters Corp.) and analyzed using LC-ESI-MS instrumentation (Waters Corp.). Mobile phases A and B were respectively made up of acetonitrile–water solution and isopropanol/acetonitrile solution, both containing 10 mM ammonium acetate and 0.1% formic acid. Bile acids were separated by an Acquity BEH C18 column (Waters Corp.) and detected using LC-ESI-MS instrumentation (Waters Corp.). Mobile phases A and B were 0.1% formic acid in water and acetonitrile, respectively. Dosages and proportions of all solvent and experimental details were performed as described.[8]

Statistical analysis

All data were presented as mean±SEM. The Student's *t* test was used for analysis of two groups, and one-way analysis of variance followed by Tukey's *post hoc* correction was used for analysis of multiple groups. Outliers were excluded from statistical analysis by outlier analysis using the ROUT method (Prism 8.0 software, GraphPad Software); $p < 0.05$ was considered to be significant.

RESULTS

Therapeutic effect of Gly-MCA on NAFLD

To determine whether Gly-MCA has a therapeutic effect on NAFL and the more progressive form NASH, mice fed a LFD or the AMLN diet for 0 to 12 weeks were then orally administered Gly-MCA for 8 weeks. Gly-MCA treatment substantially decreased body weight gain (Figure S1A), liver weights, and liver-to-body weight ratios (Figure 1A,B) compared with that of vehicle-treated mice. TG and free cholesterol contents decreased to 70.9%–85.0% and 67.9%–77.6%, respectively, in mice treated with Gly-MCA (Figure 1C,D). Gly-MCA treatment also dramatically decreased the levels of liver injury markers, ALT, and AST, compared with vehicle, even after long-term LFD feeding (Figure 1E,F). Consistently, liver histological analysis of Gly-MCA-treated mice revealed a notable reduction in hepatic steatosis with less inflammation, fibrosis, and hepatocyte necrosis (Figure 1G,H).

To further confirm the ameliorative effect of Gly-MCA on NASH, the extents of hepatic lipid metabolism, inflammation, and fibrosis gene expression were examined. Gly-MCA treatment significantly reduced the expression of fatty acid transport and anabolism-related messenger RNAs (mRNAs), such as sterol-regulatory element binding protein 1c (*Srebp1c*), cell death-inducing DNA fragmentation factor, alpha subunit-like effector A (*Cidea*), ELOVL family member 6 (*Elovl6*), stearoyl-Coenzyme A desaturase 1 (*Scd1*), and CD36 molecule (*Cd36*), and TG synthesis–related genes,
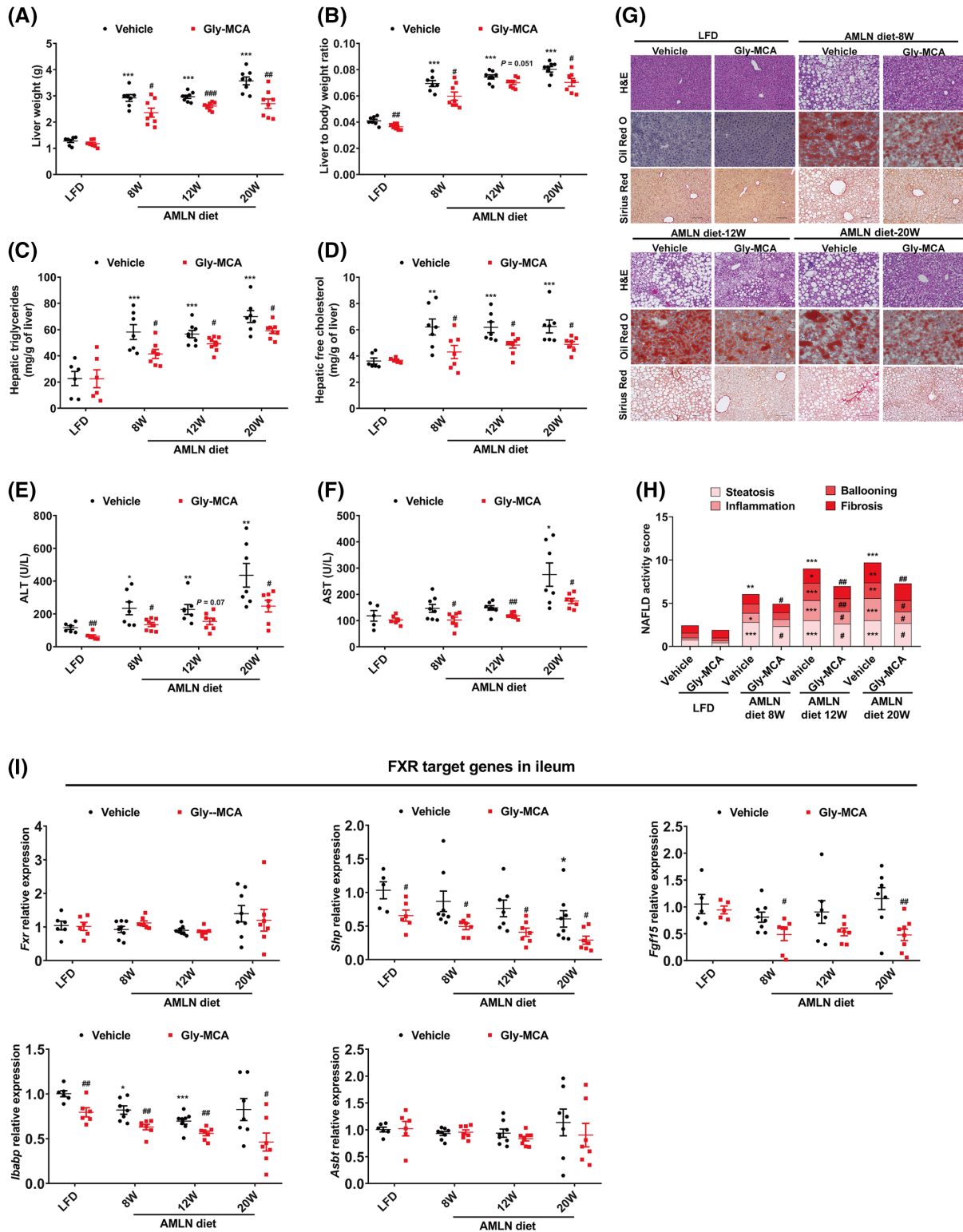
FIGURE 1 Glycine-β-muricholic acid (Gly-MCA) ameliorates the development of nonalcoholic fatty liver disease (NAFLD) and inhibits farnesoid X receptor (FXR) signaling. Mice fed a low-fat diet (LFD) or an Amylin liver NASH model (AMLN) diet for the indicated weeks were then orally administered Gly-MCA for an additional 8 weeks (n = 7–8 mice per group). (A) Liver weights. (B) Liver to body weight ratio. (C) Liver triglycerides. (D) Liver free cholesterol. (E,F) Serum alanine aminotransferase (ALT) (E) and aspartate aminotransferase (AST) (F) levels. (G) Representative hematoxylin and eosin (H&E), Oil Red O, and sirius red staining of liver sections. Scale bars, 100 μm. (H) NAFLD activity score (NAS) (n = 3–6 mice per group). (I) FXR target gene messenger RNA (mRNA) levels in ileum. Data are presented as mean ± SEM and analyzed by one-way analysis of variance (ANOVA) with Tukey's correction. *$p < 0.05$, **$p < 0.01$, and ***$p < 0.001$ compared with LFD-fed mice. #$p < 0.05$, ##$p < 0.01$, and ###$p < 0.001$ compared with vehicle-treated mice.

Abbreviations: *Asbt*, apical sodium–dependent bile acid transporter; *Fgf15*, fibroblast growth 15; *Fxr*, farnesoid X receptor; *Ibabp*, intestinal bile acid-binding protein; *Shp*, small heterodimer partner
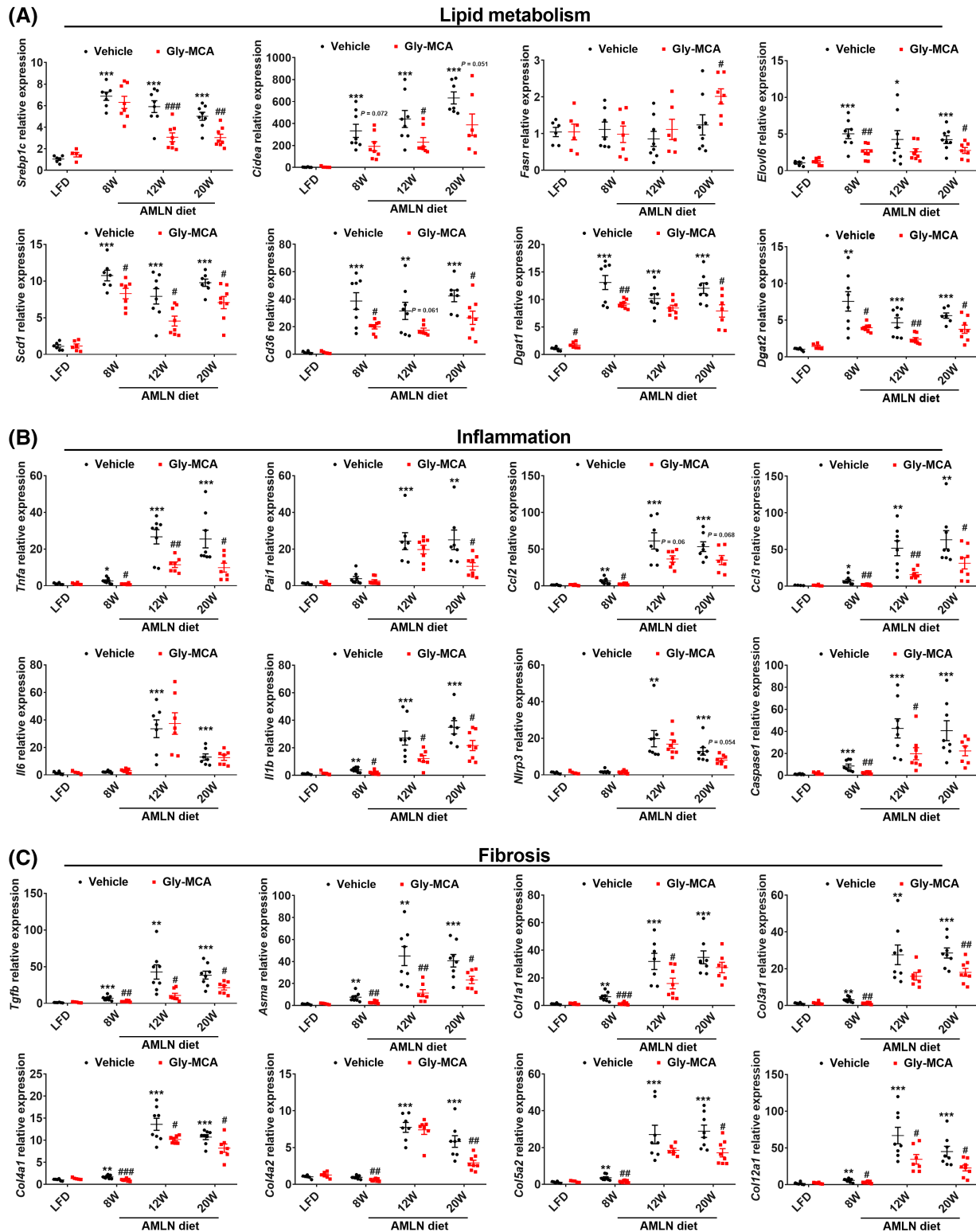
FIGURE 2 Gly-MCA decreases AMLN diet–induced hepatic steatosis, inflammation, and fibrosis. Mice fed a LFD or an AMLN diet for the indicated weeks were then orally administered Gly-MCA for an additional 8 weeks (n = 7–8 mice per group). (A) Hepatic mRNA levels of lipogenesis-related genes. (B) Hepatic mRNA levels of inflammatory cytokine and chemokine genes. (C) Hepatic mRNA levels of fibrogenesis-related genes. Data are presented as mean ± SEM and analyzed by one-way ANOVA with Tukey's correction. *$p < 0.05$, **$p < 0.01$, and ***$p < 0.001$ compared with LFD-fed mice. #$p < 0.05$, ##$p < 0.01$, and ###$p < 0.001$ compared with vehicle-treated mice. Abbreviations: *Asma*, alpha-smooth muscle actin; *Caspase1*, cysteine-asparic acid protease 1; *Ccl2*, chemokine (C-C motif) ligand 2; *Ccl3*, chemokine (C-C motif) ligand 3; *Cd36*, CD36 molecule; *Cdiea*, cell death-inducing DNA fragmentation factor, alpha subunit-like effector A; *Col1a1*, collagen, type I, alpha 1; *Col3a1*, collagen, type III, alpha 1; *Col4a1*, collagen, type IV, alpha 1; *Col4a2*, collagen, type IV, alpha 2; *Col5a2*, collagen, type V, alpha 2; *Col12a1*, collagen, type XII, alpha 1; *Dgat1*, diacylglycerol O-acyltransferase 1; *Dgat2*, diacylglycerol O-acyltransferase 2; *Elovl6*, ELOVL family member 6; *Fasn*, fatty acid synthase; *Il1b*, interleukin 1 beta; *Il6*, interleukin 6; *Nlrp3*, NLR family, pyrin domain containing 3; *Pail*, plasminogen activator inhibitor type-1; *Scd1*, stearoyl-Coenzyme A desaturase 1; *Srebp1c*, sterol-regulatory element binding protein 1c; *Tgfb*, transforming growth factor beta; *Tnfa*, tumor necrosis factor alpha

such as diacylglycerol O-acyltransferase 1 (*Dgat1*), and diacylglycerol O-acyltransferase 2 (*Dgat2*). Fatty acid synthase (*Fasn*) remained unchanged and even was increased by Gly-MCA at 20 weeks (Figure 2A). Furthermore, the AMLN diet feeding for 8, 12, and 20 weeks resulted in more frequent inflammatory cell infiltration and immune complex deposition (Figure 1G,H). Gly-MCA significantly lowered the expression of inflammatory cytokines and chemokines, manifested by reduced mRNA levels of tumor necrosis factor alpha (*Tnfa*), plasminogen activator inhibitor type-1 (*Pai1*), chemokine (C-C motif) ligand 2 (*Ccl2*), chemokine (C-C motif) ligand 3 (*Ccl3*), interleukin 1b (*Il1b*), NLR family, pyrin domain containing 3 (*Nlrp3*), and cysteine-asparic acid protease 1 (*caspase1*) (Figure 2B). Mice fed an AMLN diet exhibited hallmark features of NASH with fibrosis (Figure 1G,H), whereas Gly-MCA treatment reduced hepatic expression of mRNAs encoded by fibrogenesis-related genes, such as transforming growth factor beta (*Tgfb*), alpha-smooth muscle actin (*Asma*), collagen, type I, alpha 1 (*Col1a1*), collagen, type III, alpha 1 (*Col3a1*), collagen, type IV, alpha 1 (*Col4a1*), collagen, type IV, alpha 2 (*Col4a2*), collagen, type V, alpha 2 (*Col5a2*), and collagen, type XII, alpha 1 (*Col12a1*) (Figure 2C). These data demonstrate that Gly-MCA does not cause marked hepatotoxicity, but does decrease hepatic lipotoxicity, inflammation, and fibrosis induced by the AMLN diet.

## Gly-MCA regulates FXR signaling and decreases ceramide levels

Gly-MCA, an oral inhibitor of intestinal FXR derived from metabolites of the gut microbiota, was previously found to decrease high-fat diet (HFD)-induced obesity.[8] To verify whether Gly-MCA acts by inhibiting intestinal FXR signaling in the NASH model, we examined FXR target gene expression in the ileum and liver. Gly-MCA treatment repressed FXR signaling in the ileum, as revealed by a decrease in small heterodimer partner (*Shp*), fibroblast growth 15 (*Fgf15*), and intestinal bile acid-binding protein (*Ibabp*) mRNA levels, but not apical sodium–dependent bile acid transporter (*Asbt*) mRNA levels, suggestive that bile acid uptake was unaffected (Figure 1I). A previous study demonstrated that Gly-MCA only accumulated in the intestine and was almost undetected in the liver after oral administration,[8] so that it did not affect liver FXR signaling, which is considered beneficial to maintain hepatic lipid homeostasis. For this reason, under NASH, the hepatic FXR signaling pathway was found even activated after the treatment of Gly-MCA, as evidenced by the increased mRNAs expression of *Fxr*, *Shp*, sodium taurocholate cotransporting polypeptide (*Ntcp*) and bile salt export pump (*Bsep*), but not cytochrome P450, family 7, subfamily a, polypeptide 1 (*Cyp7a1*) mRNA levels

(Figure S2A–E), presumably at a rate independent of Gly-MCA itself, largely due to NASH remission.

Previous studies demonstrated that ceramides could facilitate the development of NASH by fueling the cellular damage caused by inflammatory cytokines, aggravating insulin resistance, and promoting mitochondrial dysfunction and oxidative stress.[15] Activation of intestine FXR promotes the mRNA expression of ceramide synthesis genes, such as sphingomyelin phosphodiesterase 3 (*Smpd3*), ceramide synthase 4 (*Cers4*), and serine palmitoyl transferase, long chain base subunit 2 (*Sptlc2*).[9,16] To further explore the mechanism underlying improved liver function phenotype by Gly-MCA, lipidomic analysis of ileum and liver metabolites was used, revealing that Gly-MCA lowered ceramide levels in both ileum and liver compared with vehicles (Figure 3A,B). Consistently, the mRNA expression levels of ileal ceramide synthesis-related genes, such as serine palmitoyl transferase, long chain base subunit 1 (*Sptlc1*), *Sptlc2*, ceramide synthase 2 (*Cer2*), *Cer4*, ceramide synthase 6 (*Cer6*), delta (4)-desaturase, sphingolipid 1 (*Degs1*), delta (4)-desaturase, sphingolipid 2 (*Degs2*), sphingomyelin phosphodiesterase 1 (*Smpd1*), sphingomyelin phosphodiesterase 2 (*Smpd2*), *Smpd3*, and sphingomyelin phosphodiesterase 4 (*Smpd4*) were measured with *Sptlc2*, *Cers4*, and *Smpd3* mRNAs being reduced by Gly-MCA (Figure 3C). These results indicate that intestinal FXR inhibition decreases intestine-derived ceramides, contributing to the Gly-MCA-improved NAFLD.

## Gly-MCA reverses mice from AMLN diet–induced NASH via the inhibition of intestinal FXR-ceramide axis

To gain a better understanding of the role of intestinal FXR in the Gly-MCA-improved NASH, control mice (*Fxr*^fl/fl) and intestine-specific *Fxr*-null (*Fxr*^ΔIE) mice were treated with either oral vehicle or Gly-MCA for 8 weeks, after 12 weeks of the AMLN diet. Gly-MCA suppressed the AMLN diet–induced increase in body weights, liver weights, and liver-to-body weight ratios in *Fxr*^fl/fl mice, but not in *Fxr*^ΔIE mice (Figure S1B, Figure 4A,B). The hepatic TG and free cholesterol contents in *Fxr*^fl/fl mice with Gly-MCA treatment were substantially lower than in vehicle-treated *Fxr*^fl/fl mice, but remained similar in *Fxr*^ΔIE mice (Figure 4C,D). Histological staining of the liver also showed that Gly-MCA decreased lipid deposition, inflammatory cell infiltration, and fibrosis in *Fxr*^fl/fl mice, with no further improvement in *Fxr*^ΔIE mice (Figure 4E,F). Gly-MCA-treated *Fxr*^fl/fl displayed lower ALT and AST compared with vehicle-treated *Fxr*^fl/fl, whereas *Fxr*^ΔIE mice were unresponsive to Gly-MCA treatment (Figure 4G,H). These results suggest that the ameliorative effects of Gly-MCA on NASH are dependent on intestinal FXR.
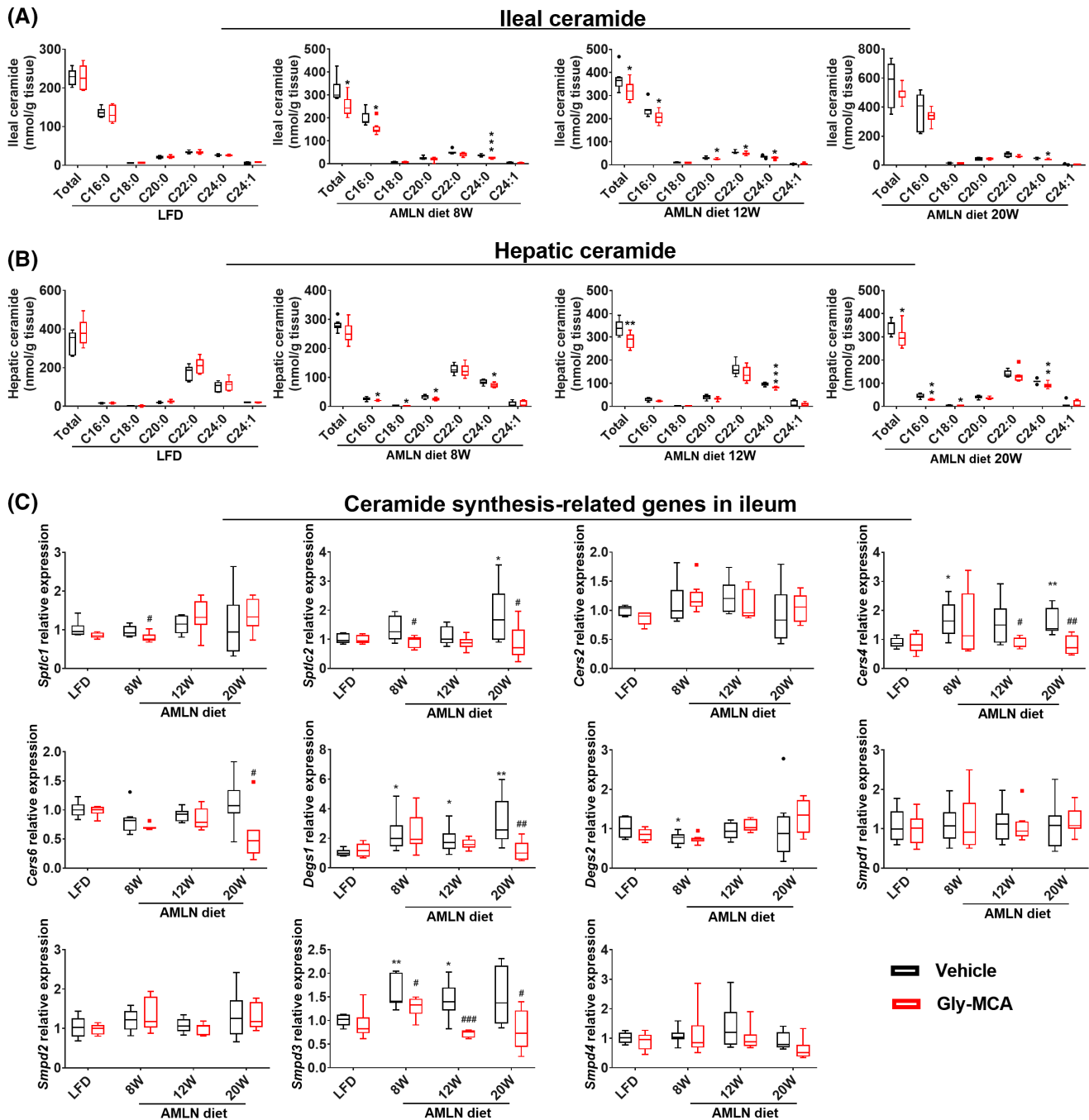
FIGURE 3 Gly-MCA decreases ileal and hepatic ceramides. Mice fed a LFD or an AMLN diet for the indicated weeks were then orally administered Gly-MCA for an additional 8 weeks (n = 7–8 mice per group). (A,B) Ileum (A) and liver (B) ceramide levels. (C) Ileal mRNA levels of ceramide synthesis-related genes. Data are presented as mean ± SEM and analyzed by one-way ANOVA with Tukey's correction. Horizon bars in the box plots indicate mean median; boxes indicate the interquartile range (IQR) between the 25th and 75th percentiles, and whiskers represent the lowest or highest values within 1.5 times IQR from the 25th or 75th quartiles. *$p < 0.05$, **$p < 0.01$, and ***$p < 0.001$ compared with vehicle-treated mice in (A) and (B) compared with LFD-fed mice in (C). #$p < 0.05$, ##$p < 0.01$, and ###$p < 0.001$ compared with vehicle-treated mice in (C). Abbreviations: *Cers2*, ceramide synthase 2; *Cers4*, ceramide synthase 4; *Cers6*, ceramide synthase 6; *Degs1*, delta (4)-desaturase, sphingolipid 1; *Degs2*, delta (4)-desaturase, sphingolipid 2; *Smpd1*, sphingomyelin phosphodiesterase 1; *Smpd2*, sphingomyelin phosphodiesterase 2; *Smpd3*, sphingomyelin phosphodiesterase 3; *Smpd4*, sphingomyelin phosphodiesterase 4; *Sptlc1*, serine palmitoyl transferase, long chain base subunit 1; *Sptlc2*, serine palmitoyl transferase, long chain base subunit 2

To further characterize the function of Gly-MCA in intestinal FXR on NASH, the mRNA levels of lipid metabolism–related (*Srebp1c*, *Cidea*, *Fasn*, *Elovl6*, *Scd1*, *Cd36*, *Dgat1*, and *Dgat2*), inflammation-related (*Tnfa*, *Pai1*, *Ccl2*, *Ccl3*, *Il6*, *Il1b*, *Nlrp3*, *caspase1*, PYD and CARD domain containing [*Pycard*], and pannexin 1 [*Panx1*]), and fibrogenesis-related (*Tgfb*, *Asma*, *Col1a1*, *Col3a1*, *Col4a1*, *Col4a2*, *Col5a2*, and
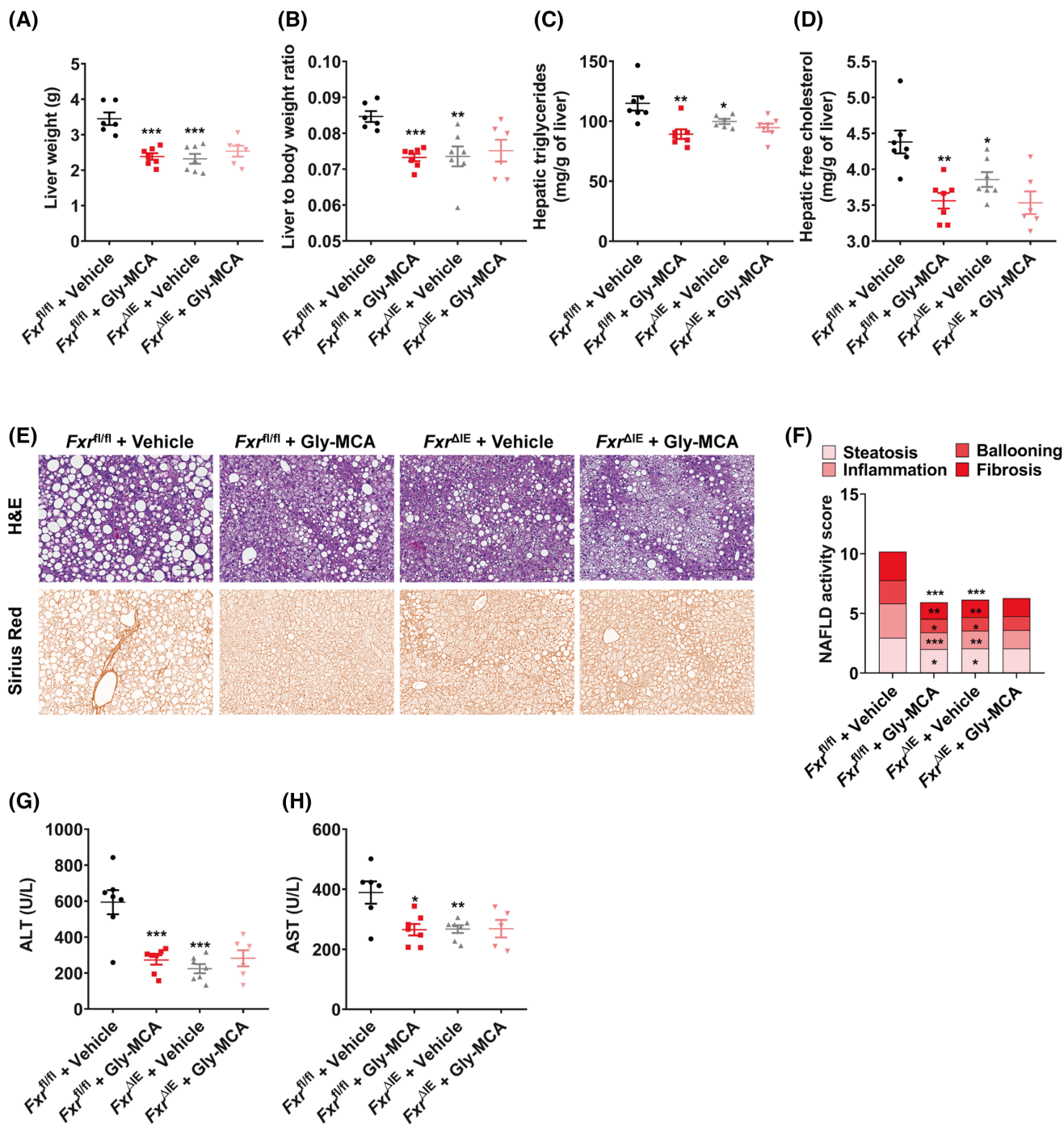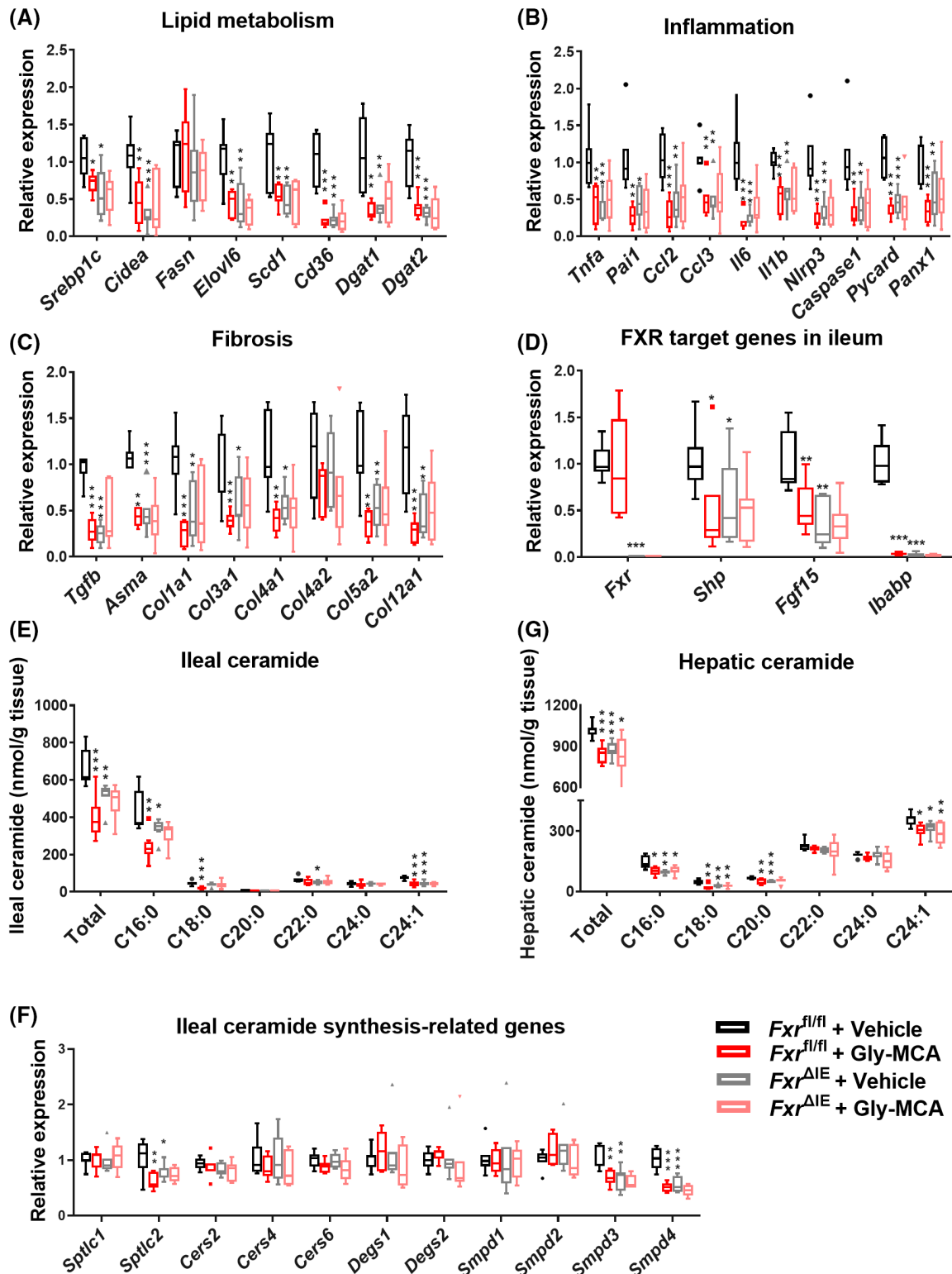
FIGURE 4 Gly-MCA improves AMLN diet–induced nonalcoholic steatohepatitis (NASH) via the inhibition of intestinal FXR. $Fxr^{fl/fl}$ and $Fxr^{\Delta IE}$ mice fed an AMLN diet for 12 weeks were then treated with vehicle or Gly-MCA for 8 weeks (n = 7 mice per group). (A) Liver weights. (B) Liver to body weight ratio. (C) Liver triglycerides. (D) Liver free cholesterol. (E) Representative H&E and sirius red staining of liver sections. Scale bars, 100 μm. (F) NAS score (n = 5 mice per group). (G,H) Serum ALT (G) and AST (H) levels. Data are presented as mean±SEM and analyzed by one-way ANOVA with Tukey's correction. *$p < 0.05$, **$p < 0.01$, and ***$p < 0.001$ compared with vehicle-treated $Fxr^{fl/fl}$ mice

Col12a1) genes were measured in the liver. Gly-MCA significantly inhibited the expression of these genes in $Fxr^{fl/fl}$ mice, except for *Fasn*, but had no further suppression in $Fxr^{\Delta IE}$ mice (Figure 5A–C). Gly-MCA showed robust inhibition of intestinal FXR signaling in $Fxr^{fl/fl}$ mice in contrast to $Fxr^{\Delta IE}$ mice

(Figure 5D). Lipidomics and quantitative PCR analysis of ileal ceramides and mRNA levels of ceramide synthesis–related genes were performed, revealing that especially the most abundant C16:0 ceramide, and *Sptlc2*, *Smpd3*, and *Smpd4* mRNA levels, were decreased in Gly-MCA-treated $Fxr^{fl/fl}$ mice

FIGURE 5 Gly-MCA ameliorates AMLN diet–induced hepatic steatosis, inflammation, and fibrosis via the inhibition of intestinal FXR-ceramide axis. $Fxr^{fl/fl}$ and $Fxr^{\Delta IE}$ mice fed an AMLN diet for 12 weeks were then treated with vehicle or Gly-MCA for 8 weeks (n = 7 mice per group). (A–C) Lipid metabolism–related (A), inflammation-related (B), and fibrogenesis-related (C) gene expression in liver. (D) Ileal mRNA levels of FXR target genes. (E) Ileal ceramide levels. (F) Ceramide synthesis–related gene mRNA levels in ileum. (G) Hepatic ceramide levels. Data are analyzed by one-way ANOVA with Tukey's correction. Horizontal bars in the box plots indicate mean median; boxes indicate IQR between the 25th and 75th percentiles, and whiskers represent the lowest or highest values within 1.5 times IQR from the 25th or 75th quartiles. *$p < 0.05$, **$p < 0.01$, and ***$p < 0.001$ compared with vehicle treated-$Fxr^{fl/fl}$ mice.
Abbreviations: *Panx1*, pannexin 1; *Pycard*, PYD and CARD domain containing
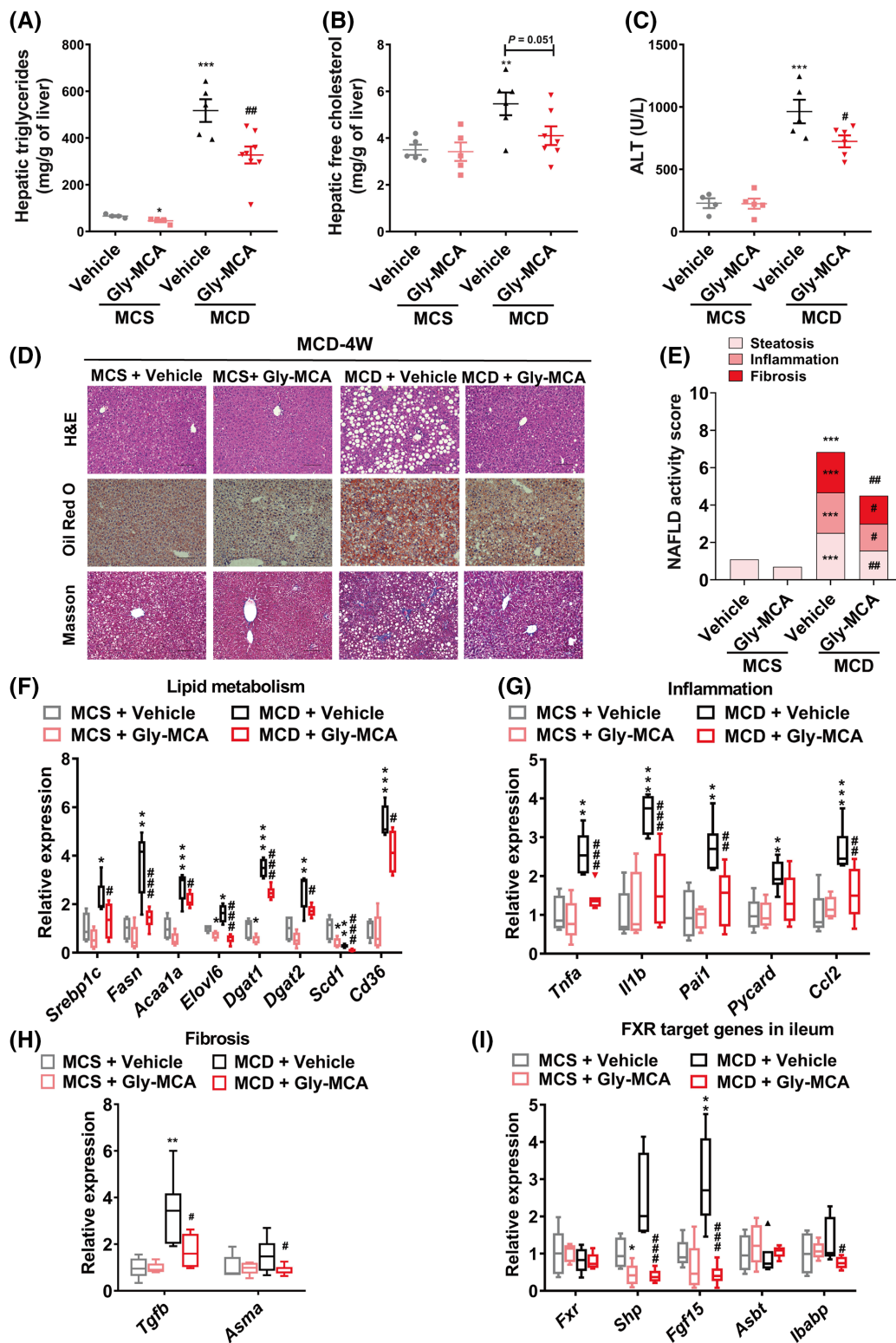
FIGURE 6 Gly-MCA prevents MCD diet–induced NASH and inhibits FXR signaling. Mice fed an methionine-choline-sufficient diet (MCS) or methionine and choline-deficient diet (MCD) for 4 weeks were concurrently treated with vehicle or Gly-MCA (n = 5–8 mice per group). (A) Liver triglycerides. (B) Liver free cholesterol. (C) Serum ALT levels. (D) H&E, Oil Red O, and Masson staining of liver sections. Scale bar, 100 μm. (E) NAS score. (F–H) Quantitative polymerase chain reaction (PCR) analysis of liver lipid metabolism–related (F), inflammation-related (G), and fibrogenesis-related (H) gene expression. (I) Quantitative PCR analysis of ileal FXR target gene mRNA expression. Data are presented as the mean±SEM and analyzed by one-way ANOVA with Tukey's correction. Horizon bars in the box plots indicate mean median; boxes indicate IQR between the 25th and 75th percentiles, and whiskers represent the lowest or highest values within 1.5 times IQR from the 25th or 75th quartiles. *$p<0.05$, **$p<0.01$, and ***$p<0.001$ compared with vehicle-treated mice for the MCS diet. #$p<0.05$, ##$p<0.01$, and ###$p<0.001$ compared with vehicle-treated mice for MCD diet. Abbreviation: *Acaa1a*, acetyl-Coenzyme A acyltransferase 1A

compared with vehicle-treated $Fxr^{fl/fl}$ mice, but not in $Fxr^{\Delta IE}$ mice (Figure 5E,F). Correspondingly, the hepatic ceramides were also reduced by Gly-MCA in $Fxr^{fl/fl}$ mice (Figure 5G). Therefore, Gly-MCA alleviates AMLN diet-induced NASH via the intestinal FXR-ceramide axis.

Gly-MCA prevents NASH development independent of adiposity

To further define whether metabolic benefits of Gly-MCA on NASH are attributable to weight loss, mice fed an MCD diet or MCS diet were concurrently treated with Gly-MCA for 4 weeks. MCD diet is used widely for establishing NASH in mice. Methionine deficiency leads to weight loss, oxidative stress, inflammation, and fibrosis, whereas choline deficiency results primarily in hepatic steatosis.[17] MCD diet feeding led to the reduced body weight compared with MCS, while Gly-MCA treatment slightly decreased body weight loss (Figure S1C). MCD diet induced an increase in the hepatic lipid contents (TG and free cholesterol), which were suppressed by Gly-MCA (Figure 6A,B). Serum ALT levels induced by the MCD diet were also decreased by Gly-MCA (Figure 6C). Histological staining of the liver revealed that Gly-MCA lowered lipid accumulation, infiltration of inflammatory cells, and fibrosis induced by the MCD diet, resulting in lower NAFLD activity scores (NAS) (Figure 6D,E). Consistently, Gly-MCA decreased the expression of mRNAs related to lipid metabolism (*Srebp1c*, *Fasn*, acetyl-Coenzyme A acyltransferase 1A [*Acaa1a*], *Elovl6*, *Dgat1*, *Dgat2, Scd1*, and *Cd36*), inflammation (*Tnfa*, *Il1b*, *Pai1*, *Pycard*, and *Ccl2*), and fibrosis (*Tgfb* and *Asma*) in the livers of MCD-fed mice (Figure 6F–H). Furthermore, Gly-MCA inhibited FXR target gene *Shp*, *Fgf15*, and *Ibabp* mRNA levels in ileum, but not in liver (Figure 6I, Figure S2F).

To further determine whether Gly-MCA prevents MCD diet–induced NASH via the inhibition of intestinal FXR, $Fxr^{fl/fl}$ and $Fxr^{\Delta IE}$ mice fed an MCD diet were concurrently treated with Gly-MCA for 4 weeks. Gly-MCA treatment significantly decreased the hepatic lipid contents (TG and free cholesterol) in $FXR^{fl/fl}$ mice, but not in $FXR^{\Delta IE}$ mice (Figure S3A,B). The serum ALT and AST levels in Gly-MCA-treated $Fxr^{fl/fl}$ mice were substantially lower compared with vehicle-treated $Fxr^{fl/fl}$ mice, whereas hepatic injury was not further alleviated in $Fxr^{\Delta IE}$ mice (Figure S3C,D). Histological staining of the liver showed that not only Gly-MCA-treated mice, but $Fxr^{\Delta IE}$ mice had substantially decreased hepatic lipid droplets, inflammatory cells, and fibrosis (Figure S3E,F). Thus, intestinal FXR plays a key and critical role in the actions of Gly-MCA on MCD-induced NASH, independent of systemic metabolic improvements.

Intestine-derived ceramides are sufficient to induce NASH

There is emerging recognition that ceramide levels are significantly and positively correlated with metabolic diseases in humans and mice.[18,19] Lipidomics analysis revealed that the MCD diet caused an increase of ceramide and bile acid levels in ileum, blood, and liver, whereas Gly-MCA decreased ceramide levels with no effects on bile acid metabolism (Figure 7A,B, Figure S4A–C). These data, together with the results from the AMLN model (Figure 3), prove that Gly-MCA prevents mice from NASH by modulating FXR signaling in intestine and reducing the intestine-derived ceramides that circulate to liver.

To more definitively establish a direct link between intestinal ceramide metabolism and NASH, C16:0 ceramide was administered by intraperitoneal injection, which was primarily absorbed into the portal vein mimicking intestine-derived ceramides, to mice fed an AMLN diet for 3 weeks. Ceramide supplementation resulted in a trend of increased liver weights and liver-to-body weight ratios, and significantly elevated TG and free cholesterol levels in the liver (Figure 7C–F). Ceramide up-regulated hepatic mRNA expression of lipid metabolism-related (*Srebp1c* and *Cd36*), inflammation-related (*Tnfa*, *Pai1*, *Ccl2*, and *Il1b*), and fibrogenesis-related (*Asma* and *Col4a1*) genes. Meanwhile, ceramide elevated mRNA expression of the endoplasmic reticulum (ER) stress-related genes, such as C/EBP-homologous protein (*Chop*) and transcription factor 4 (*Atf4*) (Figure 7G). The hepatic ER stress response *per se* exerts proinflammatory functions,[20] which could explain why ceramide more profoundly induced inflammation. These data elucidate a causal role for intestine-derived ceramides in the development of NASH.

Gly-MCA ameliorates MCD diet–induced NASH

To investigate the therapeutic effect of Gly-MCA on established NASH, mice were fed an MCD diet for 4 weeks and then treated with Gly-MCA for another 4 weeks. Gly-MCA improved hepatic lipid dysregulation, as evidenced by the significantly reduced TG and free cholesterol levels (Figure 8A,B), and volume of fat droplets in the liver (Figure 8E). H&E and Masson staining also respectively showed lesser inflammatory aggregation and collagen volume fraction in the livers of mice treated with Gly-MCA. NAS also supported these findings (Figure 8E,F). Similarly, MCD diet–induced injury was effectively alleviated by Gly-MCA in liver, as shown by lower levels of ALT and AST in the serum compared with vehicle (Figure 8C,D). These results suggest that Gly-MCA has a therapeutic effect on MCD diet–induced NASH independent of adiposity.

(A)

(B)

**(C)** **(D)** **(E)** **(F)**

(G)
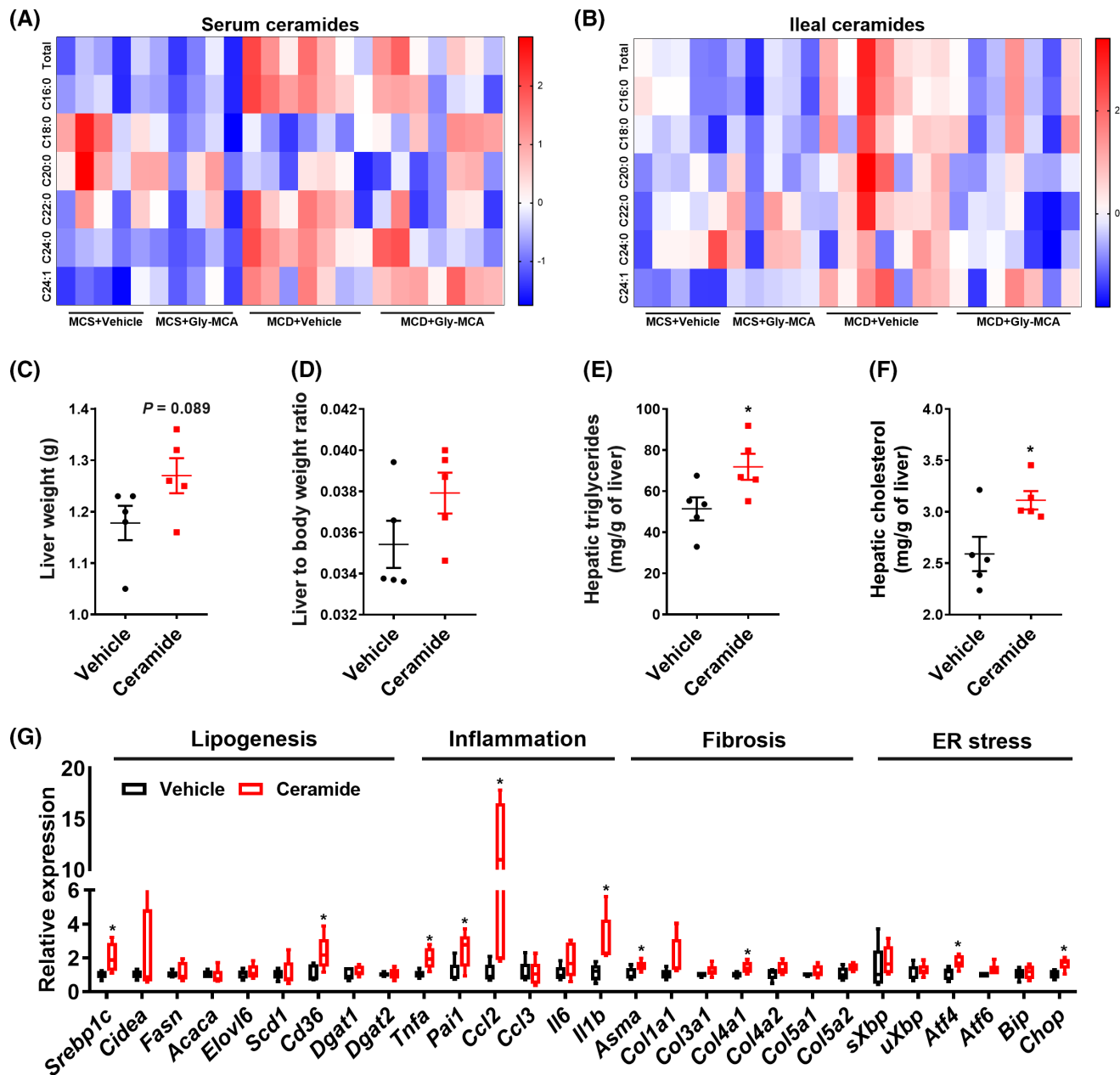
FIGURE 7 Gly-MCA prevents NASH by regulating ceramide metabolism. (A,B) Mice fed an MCS or MCD diet for 4 weeks were concurrently treated with vehicle or Gly-MCA (n = 5–8 mice per group). (A) Heat map showing the serum ceramide levels. (B) Heat map showing the ileal ceramide levels. (C–G) Mice fed an AMLN diet for 3 weeks were intraperitoneally injected with vehicle or ceramide every other day (n = 5 mice per group). (C) Liver weights. (D) Liver to body weight ratio. (E) Liver triglycerides. (F) Liver free cholesterol. (G) Quantitative PCR analysis of liver lipid metabolism-related, inflammation-related, fibrogenesis-related, and endoplasmic reticulum (ER) stress–related gene expression. (A) and (B) are normalized by z-score. (C)–(F) are presented as the mean±SEM. Horizon bars in the box plots indicate mean median; boxes indicate IQR between the 25th and 75th percentiles, and whiskers represent the lowest or highest values within 1.5 times IQR from the 25th or 75th quartiles; all data are analyzed by two-tailed Student's *t* test. *$p < 0.05$ compared with vehicle-treated mice. Abbreviations: *Acaca*, acetyl-Coenzyme A carboxylase alpha; *Atf4*, activating transcription factor 4; *Atf6*, activating transcription factor 6; *Bip*, binding immunoglobulin; *Chop*, C/EBP-homologous protein; *Xbp*, X-box binding protein

DISCUSSION

FXR is a nuclear receptor superfamily member that expressed in the intestinal epithelial cells and hepatocytes.[21] Targeting intestinal FXR constitutes a promising therapeutic approach to obesity and its metabolic complications.[22] A previous study reported that

tempol reduced the number of *Lactobacillus* species and their BSH activity in HFD-fed mice, thus giving rise to an increase in the endogenous FXR antagonist T-β-MCA.[9,11] BSH mediates the metabolic transformation of T-β-MCA to β-muricholeic acid (β-MCA), which is related to HFD-induced obesity, insulin resistance, and fatty liver.[11] Importantly, the feasibility
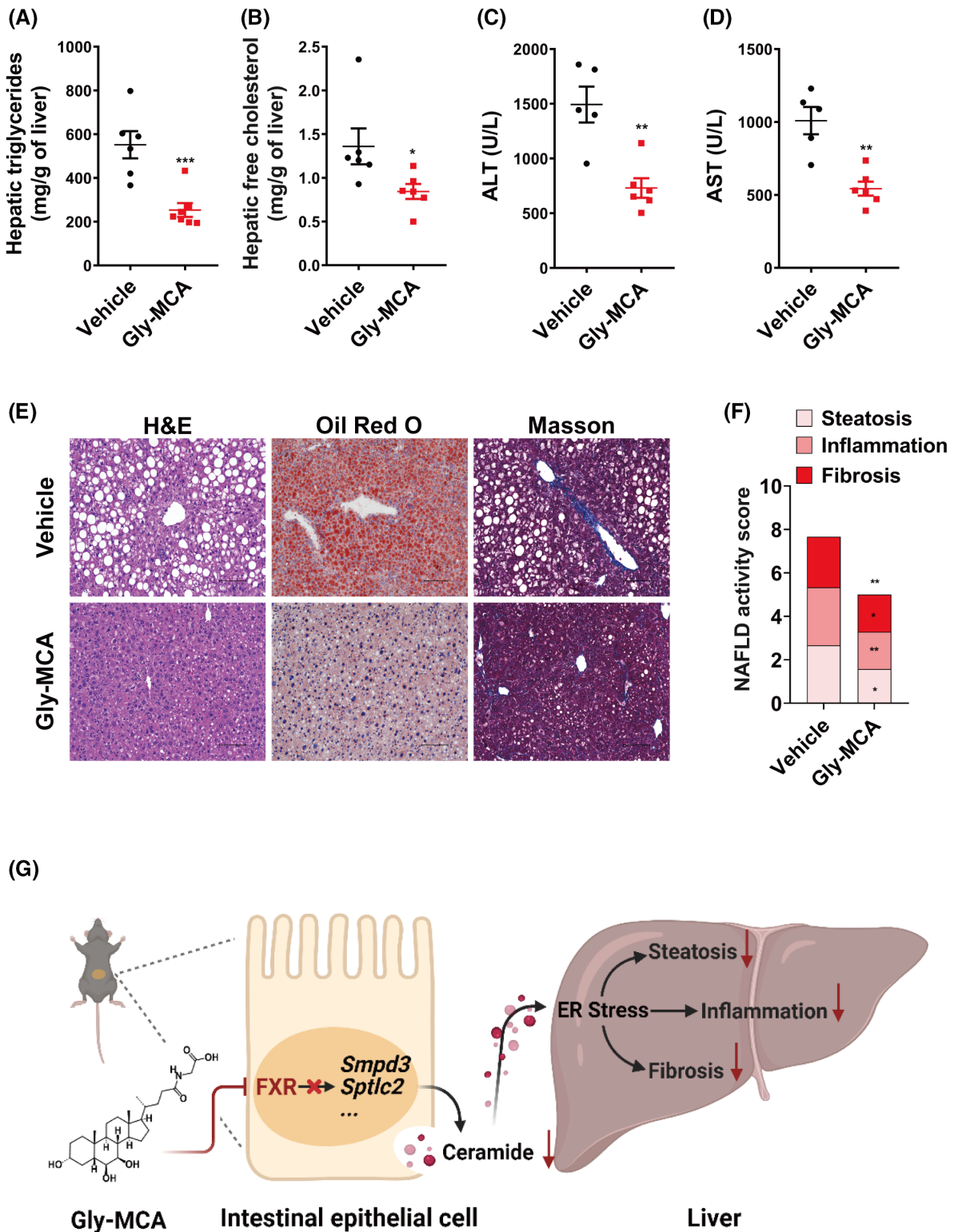
FIGURE 8 Gly-MCA ameliorates MCD diet–induced NASH. Mice fed an MCD diet for 4 weeks were then treated with Gly-MCA for 4 weeks (n = 6–7 mice per group). (A) Liver triglyceride contents. (B) Liver free cholesterol contents. (C,D) Serum ALT (C) and AST (D) levels. (E) H&E, Oil Red O, and Masson staining of liver sections. Scale bar, 100 μm. (F) NAS score (n = 6–7 mice per group). (G) Illustration summary. Gly-MCA inhibits intestinal FXR, thus down-regulating the expression of ceramide synthesis–related genes including *Smpd3* and *Sptlc2*, resulting in a decrease in ceramide levels circulating to the liver. This reduces hepatic ER stress and ameliorates NASH development, as indicated by reduced hepatic lipid accumulation, fibrosis, and especially inflammation. Data are presented as the mean ± SEM and analyzed by two-tailed Student's *t* test. *$p < 0.05$, **$p < 0.01$, and ***$p < 0.001$ compared with vehicle-treated mice

of T-β-MCA application in humans is limited, given that it and its metabolites are absent in humans. Consequently, an efficient intestine-restricted FXR antagonist is in urgent need of development. Gly-MCA has a regulatory and therapeutic potential for metabolic disorders, which is demonstrated by its improvements on obesity and insulin resistance caused by lipid accumulation.[8,13] However, the key molecular mechanisms mediating Gly-MCA treatment for NASH are still elusive. Herein, the effects of Gly-MCA on NASH was attributable to specific inhibition of the intestinal FXR-ceramide axis. Gly-MCA administration lowered ceramide synthesis in intestine by decreasing expression of the *Sptlc2* and *Cers4* genes in the *de novo* pathway, and the *Smpd3* and *Smpd4* genes in the sphingomyelinase pathway, thus reducing ceramide levels and ER stress in liver, followed by the alleviation of NASH-associated lipid accumulation, inflammation, and fibrosis in liver (Figure 8G).

Systemic activation of FXR has been shown to alleviate hepatic lipid accumulation, inflammation, and fibrosis.[23] Furthermore, activation of intestinal FXR was reported to improve insulin sensitivity and hepatic glucose metabolism.[24] However, other studies showed that specific knockout or selective inhibition of intestinal FXR improved NAFLD and obesity-related metabolic dysfunction.[8,9] Thus, intestinal FXR might exert bidirectional regulation of metabolic diseases. The current study revealed that Gly-MCA reversed and prevented NASH by decreasing hepatic lipid accumulation, inflammation, and fibrosis by suppressing intestinal FXR signaling.

Ceramides are key signaling molecules that modulate metabolic and inflammatory pathways,[25] including inducing oxidative stress, inhibiting insulin signaling, and reducing glucose uptake,[26,27] which are all potential triggers for NASH. Studies have shown that NAFLD is associated with increased expression of ceramide synthesis–related genes included in the *de novo* synthesis pathway, sphingomyelin hydrolysis pathway, and salvage pathway.[28] Pro-inflammatory cytokines like IL-1 and IL-6 increase ceramide synthesis, and ceramides conversely contribute to inflammation by reacting with TNF-α, thus forming a positive feedback regulation.[15,29] A growing body of research has proven that ceramide synthesis genes are decreased in the ileum epithelial cells by inhibiting intestinal FXR signaling.[10,30] Thus, the FXR-ceramide axis plays a crucial role in terms of regulating lipid metabolism and absorption.[31] Similarly, the present data suggest that ileal and serum ceramide levels in NASH are increased with the accumulation of TG in the liver, whereas intestine-derived ceramides promot the development of NASH. Instead, Gly-MCA reduced ileal and serum ceramide levels by inhibiting intestinal FXR signaling. Thus, Gly-MCA improved NASH by regulating the FXR-ceramide axis in the ileum.

ER is responsible for important metabolic processes in hepatocytes, including protein synthesis, transmembrane protein folding, and calcium homeostasis.[32] At the initial stage of NAFLD, lipid accumulation in the liver can cause ER stress, indicating that the pathology of NAFLD is correlated with hepatic ER dysfunction.[33] Several studies have shown that ER stress facilitates hepatic steatosis by activating the fatty acid and cholesterol synthesis–related ER transcription factors, SREBP-1c and SREBP-2,[34] which can cause a series of pathological changes to advance NAFL to NASH.[35,36] In NASH, persistent lipid deposition in hepatocytes stimulates excessive production of inflammatory factors by macrophages in which ER stress plays a significant role to promote metabolic inflammation in the liver.[37] Unfolded protein response (UPR), one of adaptive stress responses to control and alleviate ER stress, activates nuclear factor-kappa B, leading to upregulation of inflammatory factor expression, including IL-6 and TNF-α, which increases the systemic release of inflammatory factors, promoting the progress of inflammation.[38,39] The UPR signaling pathway plays a vital role in the secretion of extracellular matrix proteins, which can lead to fibrosis after excessive accumulation.[40,41] Other studies have shown that ER stress in hepatic stellate cells promotes hepatic fibrosis by protein kinase RNA-activated-like ER kinase phosphorylation[42] and the TGFβ1-SMAD signaling pathway.[43] Moreover, evidence suggests that ceramides disrupt Ca^{2+} homeostasis and activate ER-mediated pathways of apoptosis and inflammation, which causes the pathobiology of NASH.[44] In the present study, ATF-4 and its downstream CHOP, important transcriptional regulators of ER stress–mediated apoptosis,[45] were significantly upregulated by ceramides. Consistently, ceramide treatment resulted in enhanced hepatic lipid metabolism, inflammation, and fibrosis, with the most pronounced effects on inflammation in association with ceramide-induced ER stress (i.e., Gly-MCA inhibits intestinal FXR, which in turn reduces ceramide synthesis and ER stress, and thus alleviates NASH).

Recent studies have demonstrated a pivotal role of the "gut-liver" axis in NASH.[46] A key finding is that the total amount of primary bile acids increased in patients with NAFL or NASH.[47] Moreover, FXR controls the synthesis of bile acids and enterohepatic circulation by modulating the expression of genes encoding enzymes and proteins involved in bile acid synthesis and transport.[48,49] Although some bile acid transport–related genes were expressed differently in vehicle and Gly-MCA-treated NASH mice, similar bile acid pools still remaine. In the ileum, the inhibitory effect of Gly-MCA on FXR signaling suppressed the transport of bile acids across the enterocyte to the basolateral membrane by decreasing expression of IBABP, with no effects on bile acid reabsorption mediated by ASBT into the enterocytes.[50] In the liver, the ameliorative effect of Gly-MCA on NASH led to a reduction in hepatic lipotoxicity, resulting in hepatic FXR activation. Thus, improvement

of NASH by Gly-MCA was not due to altered bile acid enterohepatic circulation.

Previous studies have shown that Gly-MCA reverses and prevents obesity, focusing on elucidating its beneficial improvement of glucose and lipid metabolism.[8,13] In the current study, both the preventive and therapeutic effects of Gly-MCA on NASH were explored, and the ameliorating effects of Gly-MCA were independent of weight loss, as reflected in the reduction of lipotoxicity, inflammation, and fibrosis in liver. Furthermore, Gly-MCA improved NASH through the intestinal FXR-ceramide axis, whereas bile acid synthesis and transport were not affected, thus ruling out a direct role of bile acids in the actions of Gly-MCA on NASH. However, the present study has some limitations. Consistent with previous studies, Gly-MCA inhibited ceramide synthesis by repressing intestinal FXR signaling, accompanied by low expression of the ceramide synthesis-associated genes, such as *Sptlc2*, *Cers4*, *Smpd3*, and *Smpd4*. Nevertheless, the detailed mechanism of how FXR regulates intestinal ceramide synthesis is still unknown, hypothesizing that intestinal FXR achieves transcriptional regulation by binding to the promoters or enhancers of these genes. More critically, Gly-MCA treatment of the *Fxr*^ΔIE mouse NASH model requires further inverse validation with ceramide or FXR agonists. Finally, other mechanisms contributing to the favorable metabolic effects of Gly-MCA need to be explored, in addition to inhibiting the intestinal FXR-ceramide axis.

CONCLUSIONS

Collectively, these data reveal that Gly-MCA is a promising candidate in treating diet-induced NASH and associated phenotypes through effects on lipid metabolism by inhibiting the intestinal FXR signaling. Notably, the metabolic ameliorating effects of Gly-MCA on NASH are through the regulation of ceramide synthesis-related genes in intestine. Taken together, Gly-MCA has beneficial effects on NASH by suppressing intestinal FXR signaling and reducing ceramide-induced ER stress in liver, thus opening an avenue for the treatment of NASH.

ORCID

Frank J. Gonzalez https://orcid.org/0000-0002-7990-2140
Cen Xie https://orcid.org/0000-0002-4574-8456

REFERENCES

1. Li W, Alazawi W. Non-alcoholic fatty liver disease. Clin Med (Lond). 2020;20:509–12.
2. Kage M, Aishima S, Kusano H, Yano H. Histopathological findings of nonalcoholic fatty liver disease and nonalcoholic steatohepatitis. J Med Ultrason (2001). 2020;47:549–54.
3. Machado MV, Diehl AM. Pathogenesis of nonalcoholic steatohepatitis. Gastroenterology. 2016;150:1769–77.
4. Kitade H, Chen G, Ni Y, Ota T. Nonalcoholic fatty liver disease and insulin resistance: new insights and potential new treatments. Nutrients. 2017;9:387.
5. Buzzetti E, Pinzani M, Tsochatzis EA. The multiple-hit pathogenesis of non-alcoholic fatty liver disease (NAFLD). Metabolism. 2016;65:1038–48.
6. Younossi ZM. Non-alcoholic fatty liver disease—a global public health perspective. J Hepatol. 2019;70:531–44.
7. Sun L, Cai J, Gonzalez FJ. The role of farnesoid X receptor in metabolic diseases, and gastrointestinal and liver cancer. Nat Rev Gastroenterol Hepatol. 2021;18:335–47.
8. Jiang C, Xie C, Lv Y, Li J, Krausz KW, Shi J, et al. Intestine-selective farnesoid X receptor inhibition improves obesity-related metabolic dysfunction. Nat Commun. 2015;6:10166.
9. Jiang C, Xie C, Li F, Zhang L, Nichols RG, Krausz KW, et al. Intestinal farnesoid X receptor signaling promotes nonalcoholic fatty liver disease. J Clin Invest. 2015;125:386–402.
10. Xie C, Jiang C, Shi J, Gao X, Sun D, Sun L, et al. An intestinal farnesoid X receptor-ceramide signaling axis modulates hepatic gluconeogenesis in mice. Diabetes. 2017;66:613–26.
11. Li F, Jiang C, Krausz KW, Li Y, Albert I, Hao H, et al. Microbiome remodelling leads to inhibition of intestinal farnesoid X receptor signalling and decreased obesity. Nat Commun. 2013;4:2384.
12. Sayin SI, Wahlstrom A, Felin J, Jantti S, Marschall HU, Bamberg K, et al. Gut microbiota regulates bile acid metabolism by reducing the levels of tauro-beta-muricholic acid, a naturally occurring FXR antagonist. Cell Metab. 2013;17:225–35.
13. Zhang L, Xie C, Nichols RG, Chan SH, Jiang C, Hao R, et al. Farnesoid X receptor signaling shapes the gut microbiota and controls hepatic lipid metabolism. mSystems. 2016;1:e00070-16.
14. Kim I, Ahn SH, Inagaki T, Choi M, Ito S, Guo GL, et al. Differential regulation of bile acid homeostasis by the farnesoid X receptor in liver and intestine. J Lipid Res. 2007;48:2664–72.
15. Pagadala M, Kasumov T, McCullough AJ, Zein NN, Kirwan JP. Role of ceramides in nonalcoholic fatty liver disease. Trends Endocrinol Metab. 2012;23:365–71.
16. Tveter KM, Villa-Rodriguez JA, Cabales AJ, Zhang L, Bawagan FG, Duran RM, et al. Polyphenol-induced improvements in glucose metabolism are associated with bile acid signaling to

intestinal farnesoid X receptor. BMJ Open Diabetes Res Care. 2020;8:e001386.

17. Montandon SA, Somm E, Loizides-Mangold U, de Vito C, Dibner C, Jornayvaz FR. Multi-technique comparison of atherogenic and MCD NASH models highlights changes in sphingolipid metabolism. Sci Rep. 2019;9:16810.

18. Chavez JA, Summers SA. A ceramide-centric view of insulin resistance. Cell Metab. 2012;15:585–94.

19. Summers SA, Goodpaster BH. CrossTalk proposal: intramyocellular ceramide accumulation does modulate insulin resistance. J Physiol. 2016;594:3167–70.

20. Zhang K, Shen X, Wu J, Sakaki K, Saunders T, Rutkowski DT, et al. Endoplasmic reticulum stress activates cleavage of CREBH to induce a systemic inflammatory response. Cell. 2006;124:587–99.

21. Jiang L, Zhang H, Xiao D, Wei H, Chen Y. Farnesoid X receptor (FXR): structures and ligands. Comput Struct Biotechnol J. 2021;19:2148–59.

22. Gonzalez FJ, Jiang C, Xie C, Patterson AD. Intestinal farnesoid X receptor signaling modulates metabolic disease. Dig Dis. 2017;35:178–84.

23. Stofan M, Guo GL. Bile acids and FXR: novel targets for liver diseases. Front Med (Lausanne). 2020;7:544.

24. Wu H, Liu G, He Y, Da J, Xie B. Obeticholic acid protects against diabetic cardiomyopathy by activation of FXR/Nrf2 signaling in db/db mice. Eur J Pharmacol. 2019;858:172393.

25. Marra F, Svegliati-Baroni G. Lipotoxicity and the gut-liver axis in NASH pathogenesis. J Hepatol. 2018;68:280–95.

26. Summers SA, Nelson DH. A role for sphingolipids in producing the common features of type 2 diabetes, metabolic syndrome X, and Cushing's syndrome. Diabetes. 2005;54:591–602.

27. Argraves KM, Obeid LM, Hannun YA. Sphingolipids in vascular biology. Adv Exp Med Biol. 2002;507:439–44.

28. Longato L, Tong M, Wands JR, de la Monte SM. High fat diet induced hepatic steatosis and insulin resistance: role of dysregulated ceramide metabolism. Hepatol Res. 2012;42:412–27.

29. Holland WL, Bikman BT, Wang LP, Yuguang G, Sargent KM, Bulchand S, et al. Lipid-induced insulin resistance mediated by the proinflammatory receptor TLR4 requires saturated fatty acid-induced ceramide biosynthesis in mice. J Clin Invest. 2011;121:1858–70.

30. Qi Y, Jiang C, Cheng J, Krausz KW, Li T, Ferrell JM, et al. Bile acid signaling in lipid metabolism: metabolomic and lipidomic analysis of lipid and bile acid markers linked to anti-obesity and anti-diabetes in mice. Biochim Biophys Acta. 2015;1851:19–29.

31. Zhou Q, Song N, Wang SQ, Wang Y, Zhao YK, Zhu XD. Effect of gegen qinlian decoction on hepatic gluconeogenesis in ZDF rats with type 2 diabetes mellitus based on the farnesol X receptor/ceramide signaling pathway regulating mitochondrial metabolism and endoplasmic reticulum stress. Evid Based Complement Alternat Med. 2021;2021:9922292.

32. Gadiparthi C, Spatz M, Greenberg S, Iqbal U, Kanna S, Satapathy SK, et al. NAFLD epidemiology, emerging pharmacotherapy, liver transplantation implications and the trends in the United States. J Clin Transl Hepatol. 2020;8:215–21.

33. Lebeaupin C, Vallee D, Hazari Y, Hetz C, Chevet E, Bailly-Maitre B. Endoplasmic reticulum stress signalling and the pathogenesis of non-alcoholic fatty liver disease. J Hepatol. 2018;69:927–47.

34. Garcia-Ruiz C, Mato JM, Vance D, Kaplowitz N, Fernández-Checa JC. Acid sphingomyelinase-ceramide system in steatohepatitis: a novel target regulating multiple pathways. J Hepatol. 2015;62:219–33.

35. Wang D, Wei Y, Pagliassotti MJ. Saturated fatty acids promote endoplasmic reticulum stress and liver injury in rats with hepatic steatosis. Endocrinology. 2006;147:943–51.

36. Kim JY, Garcia-Carbonell R, Yamachika S, Zhao P, Dhar D, Loomba R, et al. ER stress drives lipogenesis and steatohepatitis via caspase-2 activation of S1P. Cell. 2018;175:133–45.e115.

37. Hotamisligil GS. Endoplasmic reticulum stress and the inflammatory basis of metabolic disease. Cell. 2010;140:900–17.

38. Song MJ, Malhi H. The unfolded protein response and hepatic lipid metabolism in non alcoholic fatty liver disease. Pharmacol Ther. 2019;203:107401.

39. Seo J, Fortuno ES 3rd, Suh JM, Stenesen D, Tang W, Parks EJ, et al. Atf4 regulates obesity, glucose homeostasis, and energy expenditure. Diabetes. 2009;58:2565–73.

40. Hussein KH, Park KM, Yu L, Kwak HH, Woo HM. Decellularized hepatic extracellular matrix hydrogel attenuates hepatic stellate cell activation and liver fibrosis. Mater Sci Eng C Mater Biol Appl. 2020;116:111160.

41. Jiang JX, Török NJ. Liver injury and the activation of the hepatic myofibroblasts. Curr Pathobiol Rep. 2013;1:215–23.

42. Koo JH, Lee HJ, Kim W, Kim SG. Endoplasmic reticulum stress in hepatic stellate cells promotes liver fibrosis via PERK-mediated degradation of HNRNPA1 and up-regulation of SMAD2. Gastroenterology. 2016;150:181–93.e188.

43. Pang Q, Jin H, Wang Y, Dai M, Liu S, Tan Y, et al. Depletion of serotonin relieves concanavalin A-induced liver fibrosis in mice by inhibiting inflammation, oxidative stress, and TGF-β1/Smads signaling pathway. Toxicol Lett. 2021;340:123–32.

44. Summers SA. Ceramides in insulin resistance and lipotoxicity. Prog Lipid Res. 2006;45:42–72.

45. Rahman K, Liu Y, Kumar P, Smith T, Thorn NE, Farris AB, et al. C/EBP homologous protein modulates liraglutide-mediated attenuation of non-alcoholic steatohepatitis. Lab Invest. 2016;96:895–908.

46. He B, Jiang J, Shi Z, Wu L, Yan J, Chen Z, et al. Pure total flavonoids from citrus attenuate non-alcoholic steatohepatitis via regulating the gut microbiota and bile acid metabolism in mice. Biomed Pharmacother. 2021;135:111183.

47. Puri P, Daita K, Joyce A, Mirshahi F, Santhekadur PK, Cazanave S, et al. The presence and severity of nonalcoholic steatohepatitis is associated with specific changes in circulating bile acids. Hepatology. 2018;67:534–48.

48. Gonzalez FJ, Jiang C, Patterson AD. An intestinal microbiota-farnesoid X receptor axis modulates metabolic disease. Gastroenterology. 2016;151:845–59.

49. Chiang JYL, Ferrell JM. Bile acid metabolism in liver pathobiology. Gene Expr. 2018;18:71–87.

50. Jia W, Xie G, Jia W. Bile acid-microbiota crosstalk in gastrointestinal inflammation and carcinogenesis. Nat Rev Gastroenterol Hepatol. 2018;15:111–28.

SUPPORTING INFORMATION

Additional supporting information can be found online in the Supporting Information section at the end of this article.